



Original article

**The Potential Ameliorative Effect of Empagliflozin on Myocardium in Cardiorenal Syndrome 3 via Targeting Mitophagy and Mitochondrial Biogenesis in Adult Male Albino Rat Model: Biochemical, Histological and Immunohistochemical Study**

Marwa Mohamed Yousry\*, Sarah Mohammed Alghandour\*

*Histology Department, Faculty of Medicine, Cairo University, Egypt\**

**Article Info**

**Article history:**

Received 12 November 2023

Accepted 28 January 2024

**Corresponding Author:**

Marwa Mohamed Yousry

[marwa.yousry@kasralainy.edu.eg](mailto:marwa.yousry@kasralainy.edu.eg)

**Keywords**

Cardiorenal syndrome 3,  
mitophagy-mitochondrial  
biogenesis,  
LC3B,  
P62,  
EMPA

**Abstract:**

**Background:** Cardiorenal syndrome-3 (CRS3) represents the pathological link between kidneys and heart where acute kidney injury (AKI) causes serious cardiac abnormalities. Disrupted mitochondrial dynamics are the main contributor to CRS3. Mitophagy plays a protective role through reducing mitochondrial damage and oxidative-stress. Empagliflozin (EMPA), a sodium-glucose cotransporter-2 inhibitor, has therapeutic effects on cardiac and renal pathology with or without diabetes type-2 through anti-oxidative, anti-inflammatory & anti-apoptotic mechanisms. **Aim of work:** Evaluating EMPA probable reparative impact on the myocardium of adult male albino rat CRS3-model using biochemical, histological & immunohistochemical studies. **Materials and Methods:** Twenty-eight adult male albino rats (3months old, 200g weight) were divided into: control

&experimental (subjected to AKI) groups. AKI-rats were subdivided equally into 3 subgroups, AKI, AKI/recovery &AKI/EMPA (received daily oral 20mg/kg EMPA 1week after renal surgery for 3weeks). **Results:** AKI induced a significant rise in serum urea, creatinine, cardiac TNF- $\alpha$ , H<sub>2</sub>O<sub>2</sub> levels, P62, cytochrome-C area percentage, besides a non-significant increase in Mn-SOD level, mitophagy-PINK1/PARKIN &mitochondrial biogenesis-PGC1 $\alpha$  gene expression, LC3B, sirtuin-3 area percentage &a significant decrease in ATP level. Myocardium showed darkly stained shrunken nuclei, disrupted transverse striations by H&E stain and minimal collagen deposition by Masson's trichrome. AKI/recovery recorded further reduction in ATP, Mn-SOD levels, PINK1/PARKIN, PGC1 $\alpha$  expression, LC3B, sirtuin-3 area percentage and evident increase in H<sub>2</sub>O<sub>2</sub> level, P62, cytochrome-C area percentage with marked myocardial affection &more collagen deposition. AKI/EMPA demonstrated an obvious improvement in the previously mentioned results. **Conclusion:** EMPA ameliorated CRS3-induced myocardial damage through the inhibition of inflammation &mitochondrial oxidative-stress in addition to mitophagy &mitochondrial biogenesis activation.

---

## 1. Introduction:

The crosstalk between kidneys and heart is the backbone that maintains metabolic waste removal, hemodynamic stability, and body functions [1]. Cardiorenal syndrome 3 (CRS3), also called acute renocardiac

syndrome, defines where an acute kidney injury (AKI) predisposes to cardiac dysfunctions [2]. AKI is considered the pathologic contributor and starter of CRS3, about 70% of patients with AKI develop CRS3 [3,4].

Several pathophysiological mechanisms, direct and indirect ones, participate in the establishment of CRS3. Direct mechanisms include oxidative stress, mitochondrial dysfunction, inflammation, apoptosis, and sympathetic nervous system activation. While indirect mechanisms are attributed to fluid overload, imbalance of electrolytes and uremic toxins [2,5]. Impaired mitochondrial function is the principal mechanism involved in promotion of both kidney and heart lesions [2] leading to myocardial infarction, acute heart failure, arrhythmia, and acute cardiogenic shock [1].

Mitophagy is a specific kind of autophagy which eliminates defective mitochondria [6]. This is through the signaling pathway phosphatase & tensin homolog- (PTEN) induced kinase 1 (PINK1) and mitochondrial E3 ubiquitin-protein ligase PARKIN (known as PARK-2, Parkinson protein 2 that was first identified in Parkinson's disease), the key receptor-independent pathway [7]. In normal situations, PINK1 is transferred into healthy mitochondria then degraded by intramembrane serine protease [8]. While during stressful conditions, PINK1 transport is impeded causing its collection on the outer mitochondria membrane that becomes phosphorylated. After that, PINK1 recruits

the activated cytoplasmic PARKIN, and further, protein P62, sequestosome 1 (SQSTM1) (one of the autophagy's selective cargo receptors), which combines with LC3 (microtubule-associated protein 1 light chain), allowing degradation of dysfunctional mitochondria and ultimately mitophagy is completed [9]. This pathway showed an influential effect on quality control of mitochondria, cellular survival, and kidney function during AKI [10,11,12].

Mitochondrial quality control, a complicated process, includes biogenesis of mitochondria, dynamics (preserving biochemical and genetic uniformity) and mitophagy (eliminating defective mitochondria). The harmony among these processes is fundamental to conserve mitochondrial number, morphology, as well as function [13]. The major organizer of mitochondrial synthesis is assigned to peroxisome proliferator-activated receptor gamma coactivator 1 alpha (PGC1 $\alpha$ ), that becomes upregulated following increased energy demands or stress conditions [14, 15], to replace the destructed mitochondria eliminated by mitophagy, in addition to repopulating the regenerating cells [16].

Sirtuin-3 (SIRT-3), a nicotinamide adenine dinucleotide, NAD<sup>+</sup>, -dependent protein deacetylase in mitochondria, is concerned with oxidative phosphorylation, and fatty

acid oxidation [17]. SIRT-3 is closely related to adenosine triphosphate (ATP) generation process through deacetylation of complexes I, II, III, & IV of mitochondria. Approximately 90% of ATP production is attributed to complexes I & III [18]. Furthermore, SIRT-3 has been shown to exhibit variable impacts in regulation of mitophagy, inhibition of cell death [19], mitochondrial biosynthesis [20] and scavenging reactive oxygen species (ROS) [21].

However, with disease progression or in cases of massive renal injury, the quantity of defective mitochondria becomes beyond the capability of mitophagy, or the mitophagy process itself becomes reduced. Thus, cellular death becomes inevitable inducing excessive tissue damage [16].

Empagliflozin (EMPA) is one of the sodium–glucose cotransporter-2 inhibitor (SGLT2i) drugs. These are hypoglycemic drugs which possess a selective inhibitory action on sodium and glucose reabsorption from proximal renal tubules, which stimulates excretion of glucose in urine, and so, reduces serum glucose levels [22]. The promising effects of SGLT2i detected in cardiovascular lesion are attributed to a diversity of mechanisms like improved glucose metabolism, decreased body weight, blood

pressure level in addition to sodium overload [23].

Although SGLT2 is selectively expressed in kidneys and very limited in heart [24], SGLT2i were recorded to exert cardioprotective effects in patients even without diabetes or hypertension [25]. Correspondingly, multiple pleiotropic effects of EMPA were shown in the aorta through intracellular signaling independent of SGLT2 [26]. Interestingly, SGLT2i were reported to possess few adverse effects and hardly lead to hypoglycemia, even in non-diabetic patients [27].

#### **Aim of work:**

The present work evaluates the role of mitophagy along with mitochondrial biogenesis on myocardium of experimentally induced CRS3 in male albino rats and the potential ameliorative impact of EMPA.

## **2. Materials and Methods:**

### **Drugs**

#### **Empagliflozin (EMPA):**

(Jardiance, supplied as tablets each including 25 mg empagliflozin, Boehringer Ingelheim Pharma GmbH & Co. KG, Biberach, Germany). The EMPA was prepared by crushing each tablet and dissolving the powder in 6.25 ml 0.9% NaCl solution [28].

## Animals

Thirty-six adult male albino rats (8 rats for pilot study and 28 rats for experimental study) of 3 months old and 200 g weight were housed in cages at  $24 \pm 1^\circ\text{C}$  in normal light/dark cycle for 2 days former to the start of the experimental study to acclimatize to the new environmental state. Then rats were maintained in the same previous situations through the whole experimental durations and allowed for regular chow as well as water *ad libitum*. This was performed in Laboratory Animal House Unit of Kasr Al-Aini, Faculty of Medicine, Cairo University and in accordance with the guidelines of Institutional Animal Care and Use Committee (IACUC), Cairo University, [approval number CU/III/F/42/23].

## Experimental Design

**This work was divided into 2 parts:**

**A) Pilot study** included 8 rats:

It was done as a former study has illustrated a relevant increase in inflammatory cytokines and cardiac cell affection at one week of unilateral renal ischemia reperfusion procedure in mice <sup>[29]</sup>, so a pilot study was conducted to verify these alterations in cardiac muscle in rats.

Four rats (model rats) were subjected to AKI, by ligation of kidneys' pedicles with clamps for bilateral renal artery and vein occlusion

for 45 min then both clamps were reopened to permit reperfusion <sup>[30]</sup>.

Four rats were used as sham rats and were subjected to the same process as AKI rats without ligation of the renal pedicles.

Following the procedure, two model rats and their corresponding sham rats were euthanized after 1 week, as well as 4 weeks (for detection of potential recovery).

**B) The experimental study** included 28 rats that were categorized into:

**Group I (control group, 10 rats):**

Rats were subdivided into:

**Subgroup Ia (2 rats):** animals were not subjected to any procedure then sacrificed after 1 and 4 weeks.

**Subgroup Ib (sham-operated) (4 rats):** that was subjected to AKI procedure of experimental group without ligation the kidneys pedicles (without bilateral renal artery and vein occlusion). Sham rats were equally euthanized 1 and 4 weeks following the procedure.

**Subgroup Ic (4 rats):** rats were subjected to same procedure as subgroup Ib then one week later, each rat was orally given 1ml of 0.9% NaCl solution, the vehicle of EMPA, on daily basis for 3 weeks <sup>[28]</sup>.

**Group II (experimental group, 18 rats):**

Briefly, anesthesia for animals was performed via intraperitoneal injection of ketamine (80 mg/kg)/xylazine (10 mg/kg) <sup>[30]</sup>

then bilateral flank incision was done to access kidneys. Renal I/R injury was applied by ligation of renal pedicles with microaneurysm clamps for 45 min for bilateral renal artery and vein occlusion. Renal ischemia was followed by reopening of clamps to allow reperfusion that was proved by the alteration in kidneys' color. Then, abdominal incisions were sutured by a 4–0 nylon monofilament thread. The rat's body temperature was carefully maintained throughout the experiment by controlling the thermostatic surgical table using a heating pad of 37 °C [30]. Postoperative antibiotic and analgesic treatments were administered by a single intramuscular injection of 24,000 UI/kg of penicillin G benzathine and subcutaneous injection of dipyron analgesic (150 mg/kg) for 3 days [31].

Following renal I/R induction the animals were randomly subdivided into three subgroups (6 rats each):

**Subgroup IIa (AKI subgroup):**

One week following renal I/R induction, the rats were sacrificed to verify the cardiac changes induced by AKI.

**Subgroup IIb (AKI/recovery subgroup):**

Following one week of AKI, rats of this subgroup received 1ml of 0.9% NaCl solution via oral gavage daily for 3 weeks.

**Subgroup IIc (AKI/ EMPA subgroup):**

Animals in this subgroup were treated as subgroup IIb, however each rat was administered 1ml of 0.9% NaCl solution containing 4mg EMPA (20mg/kg) once daily for 3 weeks through oral gavage [28].

**Animal studies**

**Serological study:**

Blood samples from each rat were collected from their tail veins immediately at the end of week 1 and 4 to assess the renal function using the enzymatic colorimetric assay to determine urea level (ab83362, United States) and creatinine level (ab65340, United States) at Biochemistry Department, Faculty of Medicine, Cairo University.

**Animal sacrifice:**

After the end of each experimental point (one and four weeks), the rats were euthanized after being anaesthetized by intraperitoneal injection of ketamine (80 mg/ kg)/xylazine (10 mg/kg) [30]. The heart of each rat was excised. Two segments (2-2.5 mm each) were obtained from apex to base of left ventricle in a level parallel to atrioventricular groove. The first slice was to prepare cardiac homogenates [32]. This was done at Biochemistry Department, Faculty of Medicine, Cairo University for ELISA, PCR, and mitochondrial studies. The second slice was processed for paraffin blocks preparation at Histology

Department, Faculty of Medicine, Cairo University.

**I. Enzyme-linked immunosorbent assay (ELISA):**

Tumour necrotic factor alpha (TNF- $\alpha$ ), a pro-inflammatory cytokine [MBS175904, MyBioSource, USA], was assessed according to the datasheet guidelines.

**II. Quantitative real-time polymerase chain reaction (qRT-PCR):**

Total RNA was isolated then complementary DNA synthesis and detection of the relative mRNA expression was done for PINK1/PARKIN (main mitophagy pathway) and PGC1 $\alpha$  (crucial regulator of mitochondria biosynthesis) using the primers and the Rotor Gene 6000 series software version 1.7 (Corbett Life Science, USA). Then the relative expression of genes was studied as a normal ratio to beta actin (internal control). The primer PCR sequences used were:

PINK1: Forward 5'-CATGGCTTTGGATGGAGAGT-3'

Reverse 5'-TGGGAGTTTGCTCTTCAAGG-3'

PARKIN: Forward 5'-CTGGCAGTCATTCTGGACAC-3'

Reverse 5'-CTCTCCACTCATCCGGTTTG-3'

PGC1 $\alpha$ : Forward 5'-AAACTTGCTAGCGGTCCTCA-3'

Reverse 5'-TGGCTGGTGCCAGTAAGAG-3'

Beta actin: Forward: 5'-GGCATCCTGACCCTGAAGTA-3'

Reverse: 5' - GGGGTGTTGAAGGTCTCAA-3'

**III. Mitochondrial isolation:**

Isolation of mitochondria from heart was done by centrifugation according to described method of Gumustaz et al., 2006<sup>[33]</sup>. Then, according to guidelines of manufacturer, the following was assessed:

- ATP content using ATP Assay Kit, (Beyotime, China).
- Hydrogen peroxide (H<sub>2</sub>O<sub>2</sub>) level using Amplex Red reagent (Invitrogen), an indicator of oxidative stress.
- Manganese superoxide dismutase, Mn-SOD, (a special type of SOD in mitochondria, its activity represents the cell's capacity to remove mitochondrial superoxide)<sup>[34]</sup>. It was measured using Mn-SOD activity Assay Kit with WST-8 (Beyotime, China).

**IV. Histological Study**

**Paraffin block preparation:**

Cardiac slices were fixed by keeping them for one day in 10% formol saline, then the specimens were prepared to paraffin blocks. Six  $\mu\text{m}$ -thick sections were sliced then stained with:

**1- Hematoxylin and Eosin stain (H&E)**

<sup>[35]</sup>: To illustrate structure and alterations of myocardium.

**2- Masson's trichrome stain** <sup>[35]</sup>: To visualize collagen fibers.

**3- Immunohistochemical staining for:**

- a. LC3B**, microtubule-associated protein 1-light chain 3 beta, [rabbit polyclonal antibody, ab48394, abcam, USA]: a form of LC3II, represents one of the structural proteins of autophagosome, and considered as an autophagosome marker <sup>[36]</sup> that appears as cytoplasmic reaction.
- b. SQSTM1/P62**, sequestosome 1, protein P62, [rabbit polyclonal antibody, ab91526, abcam, USA]: a substrate of LC3 <sup>[9]</sup> which appears as positive reaction in the cytoplasm.
- c. SIRT-3**, sirtuin-3 [rabbit polyclonal antibody, ab189860, abcam, USA]: a NAD<sup>+</sup> dependent protein deacetylase that regulates mitochondrial target proteins <sup>[17]</sup>. It appears as cytoplasmic immunoreactivity.

**d. Cytochrome C** [rabbit polyclonal antibody, ab90529, abcam, USA]: an initiator of apoptosis through its leakage from mitochondria to cytoplasm <sup>[37]</sup>. It appears as cytoplasmic immunostaining.

- Immunostaining was performed by avidin-biotin technique <sup>[35]</sup>:

1- Boiling of cardiac sections was applied in 10 mM citrate buffer (cat no 005000) for 10 min at pH 6 for antigen retrieval.

2- This was followed by cooling the cardiac sections at standard temperature for 20 min.

3-Incubation with primary antibodies was performed for 60 min. According to manufacturer's datasheet, optimal recommended dilutions were 1/200 - 1/400 for LC3B antibody, 2 - 5  $\mu\text{g}/\text{ml}$  for SQSTM1/P62 antibody, 1/20 - 1/50 for SIRT-3 antibody, and 1  $\mu\text{g}/\text{ml}$  for cytochrome C antibody.

4- Immunostaining was accomplished by utilizing Ultravision One Detection System (cat no TL - 060- HLJ) and Lab Vision Mayer's hematoxylin counterstaining (cat no TA- 060- MH).

The following materials: Citrate buffer, Ultravision One Detection System along with Ultravision Mayer's hematoxylin were bought from Labvision, ThermoFisher scientific, USA.

The positive control for LC3B and SQSTM1/P62 appeared as cytoplasmic immunoreaction in the brain tissue and heart respectively. Regarding SIRT-3, the positive control was kidney tissue and that of cytochrome C was skeletal muscle with positive immunoexpression in cytoplasm. While the negative control cardiac sections were submitted to the prior steps without adding the primary antibodies.

#### **V. Morphometric study**

Using Leica Qwin-500 LTD-software image analysis computer system (Cambridge, England) connected to a light microscope with a colored video camera, the area percent of collagen fibers in Masson's trichrome-stained sections as well as the area percent of positive immunoreactivity of LC3B, P62, SIRT-3 and cytochrome C were measured in the corresponding immunostained sections. This was done in 10 non-overlapping areas for each animal in each group ( $\times 100$ ) using the binary mode.

#### **VI. Statistical analysis**

All biochemical and morphometric results were analyzed using IBM Statistical Package for the Social Sciences (SPSS) version 21. This was achieved by one-way analysis of

variance (ANOVA) and "Tukey" post hoc test. The findings were illustrated as mean  $\pm$  standard deviation and were regarded significant when probability value was  $< 0.05$  [38].

All the histological and morphometric studies were accomplished at the Histology Department, Faculty of Medicine, Cairo University.

### **3. Results:**

#### **General observations**

- No deaths were noticed in all experimental rats.
- Rats of subgroups Ia, Ib and Ic exhibited the same biochemical, and histological results; therefore, they were all described as control (group I).

#### **Biochemical Results**

- Renal function tests (serum urea, and creatinine) [Figs. 1a&1b] and cardiac TNF- $\alpha$  [Fig. 1c] displayed significant rise in subgroups IIa and IIb versus group I. As regards subgroup IIb, non-significant reduction was recorded in relation to subgroup IIa. Whereas there was significant reduction in subgroup IIc versus IIb and non-significant elevation as compared to group I.
- Mitochondrial levels of ATP [Fig. 1d] revealed significant decrease in subgroup

IIa and subgroup IIb compared to group I. As well, subgroup IIb recorded significant low values as compared to subgroup IIa. On the contrary, subgroup IIc showed significant increase in comparison to subgroup IIb and significant decrease versus the control group.

- Mitochondrial  $H_2O_2$  [**Fig. 1e**] showed significant high values in subgroup IIa and subgroup IIb versus control group. Additionally, there was significant rise in subgroup IIb versus subgroup IIa. However, subgroup IIc demonstrated significant diminution compared to subgroup IIb and significant increase compared to control.
- Regarding the Mn-SOD activity [**Fig. 1f**] and the relative mRNA expressions of mitophagy associated markers (PINK1 and PARKIN), together with biogenesis marker, PGC1 $\alpha$ , [**Figs. 1g, 1h & 1i respectively**] non-significant increase was recorded in subgroup IIa versus group I. In addition, subgroup IIb illustrated a significant decrease versus subgroup IIa and group I. However, a significant rise in subgroup IIc versus subgroup IIb and significant decrease compared to group I were detected.

## **Histological Results**

### **H&E-stained sections**

In **control group** [**Fig. 2a**], longitudinally cut cardiac muscle was composed of cylindrical branched cardiac muscle fibers with acidophilic sarcoplasm and transverse striations. Each cardiomyocyte had a single central oval nucleus with prominent nucleolus and joined with other cardiomyocytes with intercalated discs. Connective tissue (CT) endomysium contained vascular network seen between cardiac muscle fibers.

However, in **subgroup IIa (AKI subgroup)** [**Fig. 2b**] some myocardial fibers showed darkly stained shrunken nuclei, focal areas of degeneration comprising disrupted myofibrils and transverse striations, and interrupted intercalated discs. Additionally, apparently widened CT endomysium with inflammatory infiltration was observed.

**Subgroup IIb (AKI/recovery subgroup)** [**Figs. 2c&2d**], showed disrupted histological architecture of multiple muscle fibers. They were illustrated as focal areas of degeneration in the sarcoplasm with lost transverse striations, multiple pyknotic nuclei, and disrupted intercalated discs. In addition to the presence of widened CT endomysium that was occupied by inflammatory cell

infiltration and multiple elongated fibroblasts like cells.

Concerning **subgroup IIc (AKI/EMPA subgroup)** [Fig. 2e], apparent improvement of cardiac muscle histological alterations was illustrated. However, some muscle fibers showed pyknotic nuclei and scarce focal areas of degeneration with disrupted transverse striations. CT endomysium showed very few inflammatory cells.

#### **Masson's trichrome-stained sections**

**Control group** [Fig. 3a] and **subgroup IIa (AKI subgroup)** [Fig. 3b] showed minimal collagen deposition in the CT endomysium among the muscle fibers. However, **subgroup IIb (AKI/recovery subgroup)** [Fig. 3c] exhibited apparent increase in collagen fibers amount that was decreased in **subgroup IIc (AKI/EMPA subgroup)** [Fig. 3d].

#### **LC3B immunostained sections**

The negative control myocardial sections [Fig. 4a] without adding the LC3B primary antibody demonstrated negative immunoreaction.

The **group I (control group)** [Fig. 4b] and **subgroup IIa (AKI subgroup)** [Fig. 4c], showed profuse positive cytoplasmic immunoreactivity in cardiac muscle fibers. Such immunoreaction was regressed in

multiple cardiac muscle fibers of **subgroup IIb (AKI/recovery subgroup)** [Fig. 4d]. While prominent positive cytoplasmic immunoreactivity was expressed in most cardiac muscle fibers in **subgroup IIc (AKI/EMPA subgroup)** [Fig. 4e].

#### **P62 immunostained sections**

The negative control cardiac sections [Fig. 5a] showed negative immunostaining when omitting the addition of P62 primary antibody.

In **group I (control group)** [Fig. 5b], the positive immunoreaction was sparse in the cytoplasm of muscle fibers. This immunoreaction was illustrated in some fibers in **subgroup IIa (AKI subgroup)** [Fig. 5c]. On the other hand, **subgroup IIb (AKI/recovery subgroup)** [Fig. 5d] displayed an apparent increase in the positive immunoreaction. Such immunoreactivity was few in cardiac muscle fibers of **subgroup IIc (AKI/EMPA subgroup)** [Fig. 5e].

#### **SIRT-3 immunostained sections**

The negative control myocardial sections [Fig. 6a] after skipping SIRT-3 primary antibody illustrated negative immunoreactivity.

**Group I** [Fig. 6b] and **subgroup IIa (AKI subgroup)** [Fig. 6c] showed widely

distributed cytoplasmic positive immunoreaction in cardiac muscle fibers. While a few areas of cytoplasmic immunoreaction were noticed in **subgroup IIb (AKI/recovery subgroup)** [Fig. 6d]. As regards **subgroup IIc (AKI/EMPA subgroup)** [Fig. 6e] abundant positive immunoreactivity in muscle fibers cytoplasm was observed.

### **Cytochrome C immunostained sections**

Regarding the negative control of myocardium sections [Fig. 7a], negative immunoreaction was demonstrated with omitting the step of adding cytochrome C primary antibody.

The **group I (control group)** [Fig. 7b] demonstrated scarce positive cytoplasmic immunoreactivity in very few cardiac muscle fibers. However, multiple cardiac muscle fibers showed positive cytoplasmic immunoreactivity in **subgroup IIa (AKI subgroup)** [Fig. 7c] that appeared widespread in **subgroup IIb (AKI/recovery subgroup)** [Fig. 7d], then was limited to some fibers in **subgroup IIc (AKI/EMPA subgroup)** [Fig. 7e].

### **Morphometric Results**

Statistically, the mean area percent of collagen fibers in Masson's trichrome-stained sections [Fig. 3e] showed non-significant elevation in subgroup IIa versus control. However, subgroup IIb exhibited a significant increase versus control and subgroup IIa. As regards subgroup IIc, a significant reduction versus subgroup IIb and non-significant rise versus the control were demonstrated.

Concerning, the mean area percent of LC3B [Fig. 4f] as well as SIRT-3 [Fig. 6f], positive immunoreactivity exhibited non-significant increase in subgroup IIa and significant diminution in subgroup IIb versus group I. While a significant low value was noticed in subgroup IIb versus subgroup IIa. Subgroup IIc displayed significant increase versus subgroup IIb and significant decrease versus group I.

P62 [Fig. 5f] and cytochrome C [Fig. 7f] positive immunoreactions' mean area percent displayed significant increase in subgroups IIa & IIb as opposed to control group. Moreover, a significant increase was observed in subgroup IIb versus subgroup IIa. While in subgroup IIc, there was significant reduction versus subgroup IIb and significant elevation versus group I.

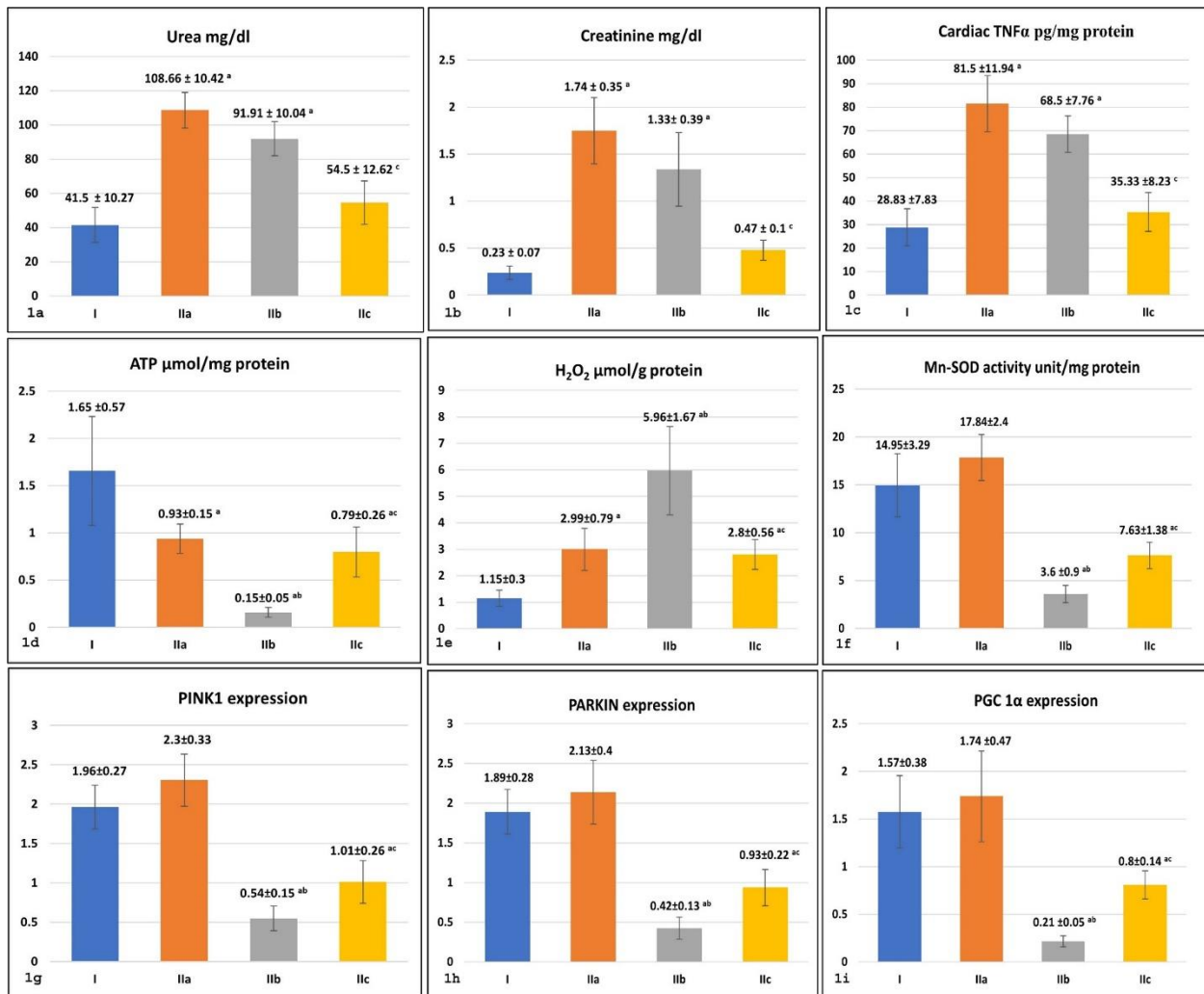


**Figure 1: Histogram illustrating mean values of:**

**1a,1b &1c:** Serum urea & creatinine and cardiac TNF-α levels.

**1d,1e&1f:** Mitochondrial ATP, H<sub>2</sub>O<sub>2</sub> and Mn-SOD activity levels.

**1g,1h&1i:** PINK1, PARKIN and PGC1 α relative mRNA expressions.

[<sup>a</sup> as compared to group I, <sup>b</sup> as compared to subgroup IIa & <sup>c</sup> as compared to subgroup IIb (significant difference at  $P < 0.05$ )]

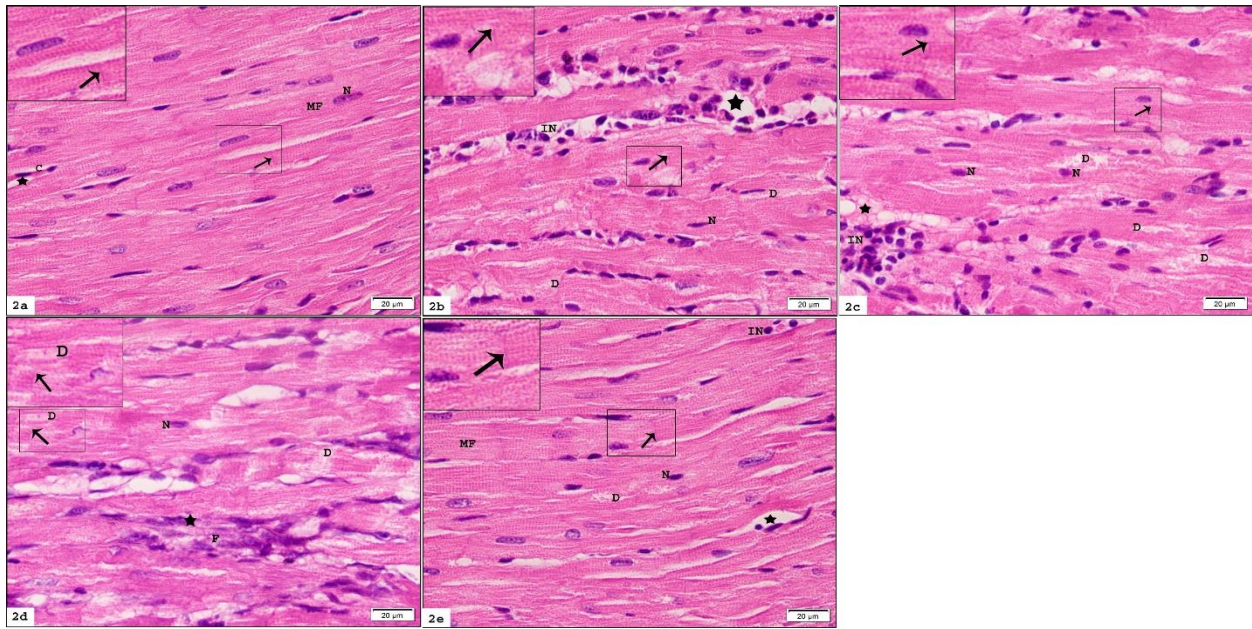


**Figure 2: Photomicrographs of H&E-stained longitudinal sections of cardiac muscle:**

**2a (group I, control group):** Illustrating cylindrical branched muscle fibers (MF) consist of cardiomyocytes joined together with intercalated discs (arrow). Each cardiac cell exhibits acidophilic sarcoplasm with transverse striations and a single oval central nucleus (N) with prominent nucleolus. CT endomysium (star) is seen between cardiac muscle fibers containing capillary network (C).

**2b (subgroup IIa, AKI subgroup):** Showing some muscle fibers that appeared with shrunken darkly stained nuclei (N), focal areas of degeneration (D) of disrupted myofibrils and transverse striations, and interrupted intercalated discs (arrow). Apparently, the CT endomysium appears widened (star) with inflammatory cell infiltration (IN).

**2c&2d (subgroup IIb, AKI/recovery subgroup):** Illustrating multiple muscle fibers having small darkly stained nuclei (N), focal areas of degeneration (D) with lost transverse striations, and interrupted intercalated discs (arrow). CT endomysium is widened (star) containing inflammatory cell infiltration (IN) (in 2c) and multiple elongated fibroblasts like cells (F) (in 2d).

**2e (subgroup IIc, AKI/EMPA subgroup):** Apparently ameliorated histological architecture is noted in cardiac muscle fibers (MF) that formed of cardiac myocytes joined by intercalated discs (arrow). In addition to the presence of some shrunken deeply stained nuclei (N), sparse focal areas of degeneration (D) with disrupted transverse striations and very few inflammatory cells (IN) in CT endomysium (star).

[H&E, x400&inset x1000]

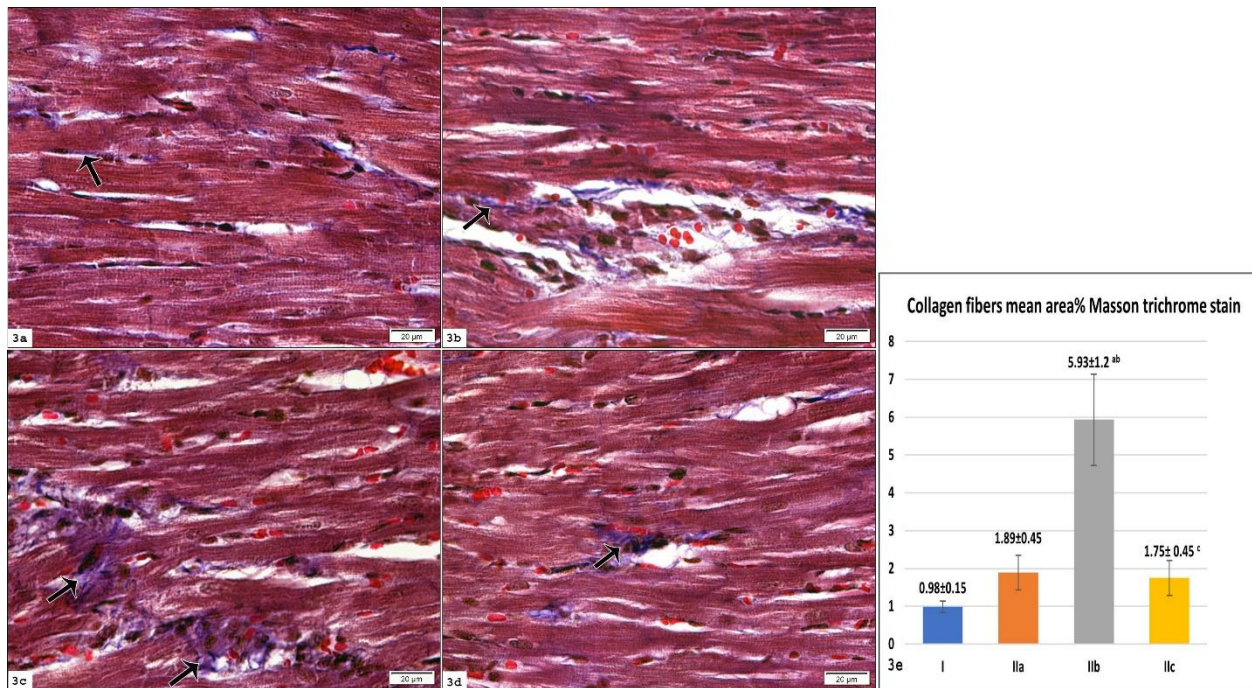


**Figure 3: Photomicrographs of Masson's trichrome stained myocardium sections:**

**3a (control group) and 3b (AKI subgroup):** Minimal collagen fibers deposition (arrow) is detected in connective tissue endomysium between the muscle fibers.

**3c (AKI/recovery subgroup):** The amount of collagen fibers deposition (arrows) is apparently increased.

**3d (AKI/EMPA subgroup):** There are some collagen fibers depositions (arrow) noticed between muscle fibers.

[Masson's trichrome stain, x400].

**3e: Histogram demonstrating the mean area % of collagen fibers. [<sup>a,b& c</sup> as compared to group I, subgroups IIa & IIb respectively (significant difference at  $P < 0.05$ )]**

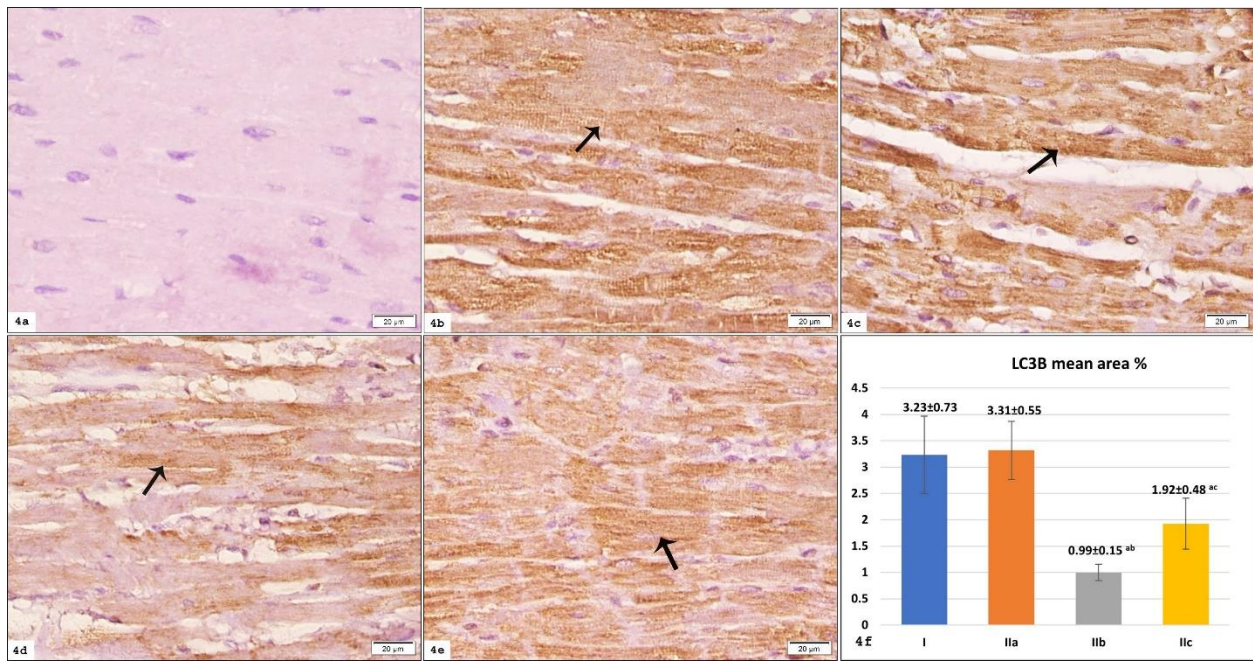


**Figure 4: Photomicrographs of LC3B immunostained cardiac muscle sections:**

**4a negative control cardiac sections** after omitting the LC3B primary antibody showing negative immunostaining.

**4b (Group I) and 4c (AKI subgroup):** Abundant positive cytoplasmic immunostaining (arrow) is observed in cardiac muscle fibers.

**4d (AKI/recovery subgroup):** Exhibits markedly reduced positive cytoplasmic immunostaining (arrow) in multiple muscle fibers.

**4e (AKI/EMPA subgroup):** Positive cytoplasmic immunoreactivity (arrow) is prominent in most of cardiac muscle fibers.

[anti LC3B immunohistochemical stain, x400].

**4f:** Histogram showing the mean area % of LC3B positive immunoreaction. [<sup>a,b& c</sup> as compared to group I, subgroups IIa & IIb respectively (significant difference at  $P < 0.05$ )]

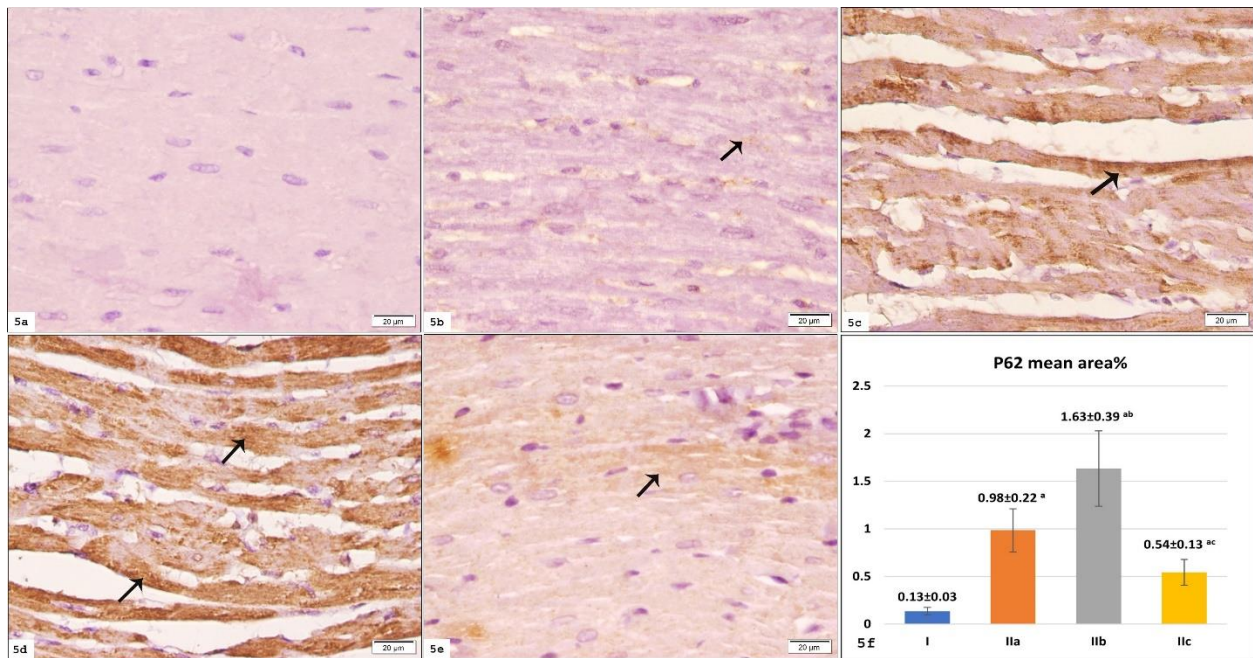


**Figure 5: Photomicrographs of P62 immunostained cardiac muscle sections:**

**5a negative control cardiac sections** after skipping the P62 primary antibody step showing negative immunoreaction.

**5b (Group I):** Barely noted positive immunostaining (arrow) in cytoplasm of myocardium fibers.

**5c (AKI subgroup):** Shows some positive cytoplasmic immunoreaction (arrow) in muscle fibers.

**5d (AKI/recovery subgroup):** An obvious increase in positive immunoreaction (arrows) is illustrated in myocardial fibers' cytoplasm.

**5e (AKI/EMPA subgroup):** Positive immunoreactivity (arrow) is noticed in the cytoplasm of few muscle fibers.

[anti P62 immunohistochemical stain, x400].

**5f:** Histogram illustrating the mean area % of P62 positive immunoreaction. [<sup>a,b& c</sup> as compared to group I , subgroups IIa & IIb respectively (significant difference at  $P < 0.05$ )]

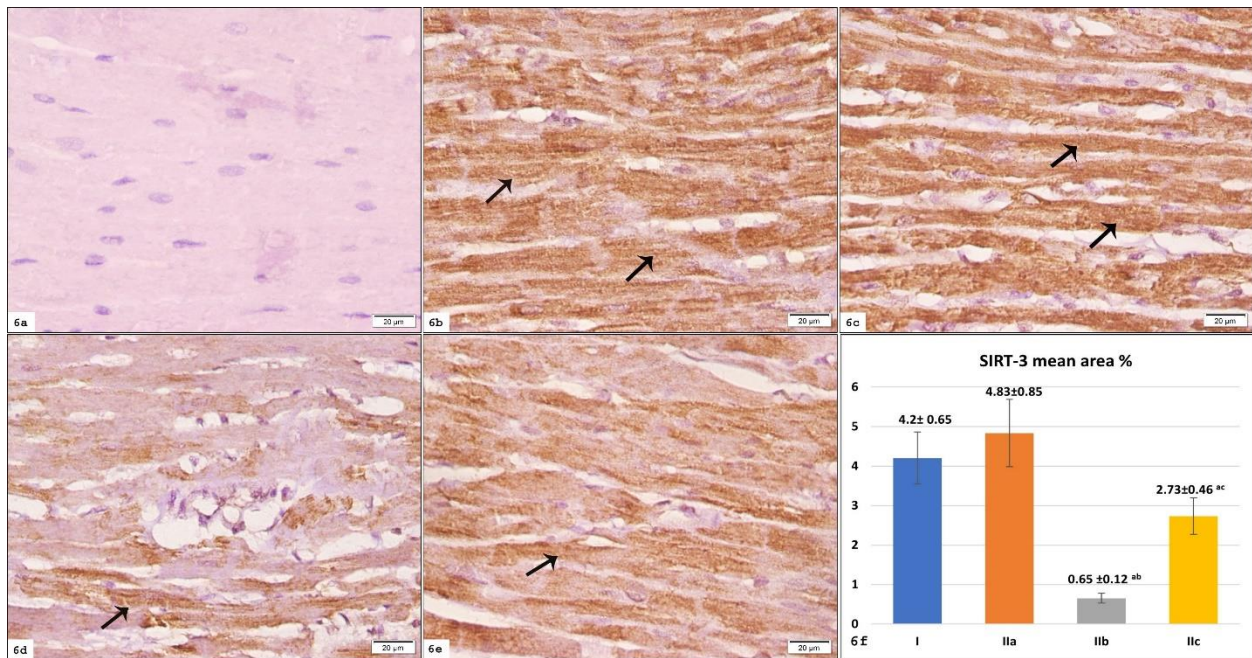


**Figure 6: Photomicrographs of SIRT-3 immunostained cardiac muscle sections:**

**6a negative control sections of myocardium** without adding the SIRT-3 primary antibody showing negative immunoreaction.

**6b (Group I) and 6c (AKI subgroup):** Illustrating widespread positive cytoplasmic immunoreaction (arrows) in cardiac muscle fibers.

**6d (AKI/recovery subgroup):** The positive cytoplasmic immunoreaction (arrow) is confined to few cardiac muscle fibers.

**6e (AKI/EMPA subgroup):** The positive cytoplasmic immunostaining (arrow) is profuse in many cardiac muscle fibers.

[anti SIRT-3 immunohistochemical stain, x400].

**6f:** Histogram demonstrating the mean area % of SIRT-3 positive immunoreaction. [a,b& c as compared to group I, subgroups IIa & IIb respectively (significant difference at  $P < 0.05$ )]

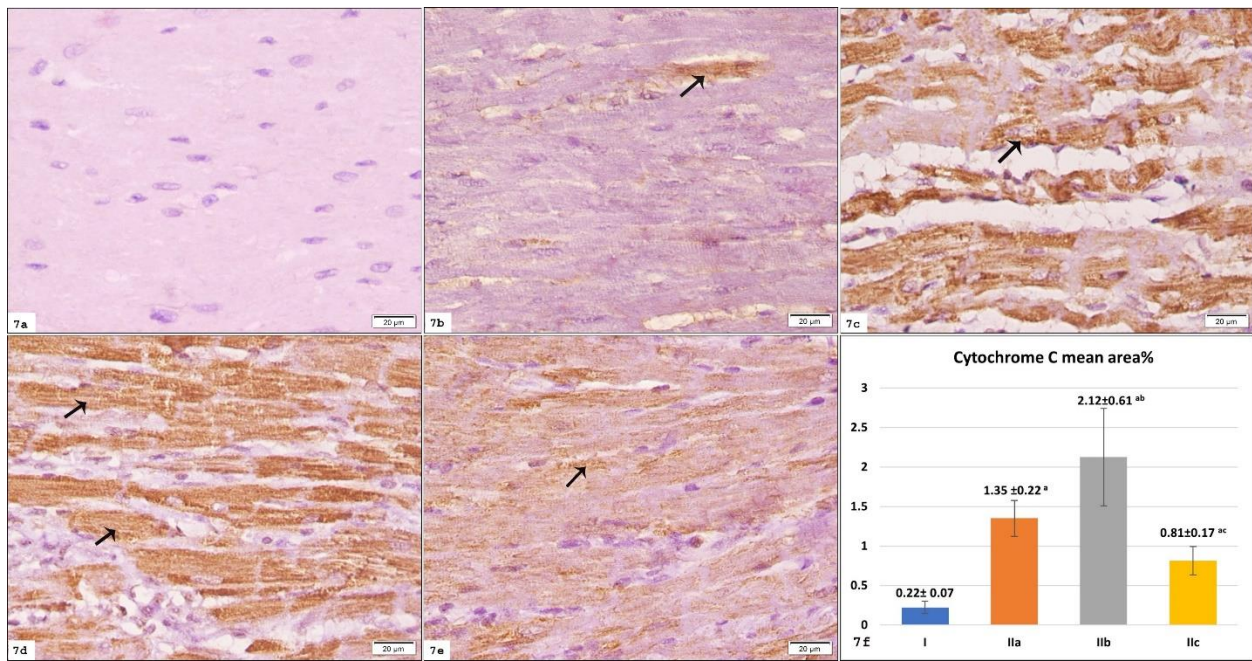


**Figure 7: Photomicrographs of cytochrome C immunostained cardiac muscle sections:**

**7a negative control sections of heart tissue** without addition of the cytochrome C primary antibody showing negative immunostaining.

**7b (Group I):** The positive cytoplasmic immunoreaction (arrow) appears in sparse cardiac muscle fibers.

**7c (AKI subgroup):** The positive cytoplasmic immunoreaction (arrow) is considerable in many cardiac fibers.

**7d (AKI/recovery subgroup):** There is widely distributed positive cytoplasmic immunoreaction (arrows) in most cardiac muscle fibers.

**7e (AKI/EMPA subgroup):** Positive cytoplasmic immunoreactivity (arrow) is noted in some muscle fibers.

[anti cytochrome C immunohistochemical stain, x400].

**7f:** Histogram showing the mean area % of cytochrome C positive immunoreaction. [<sup>a,b&c</sup> as compared to group I, subgroups IIa & IIb respectively (significant difference at  $P < 0.05$ )]

#### **4. Discussion:**

Renal ischemia-reperfusion (I/R) injury is related to diverse clinical as well as operative settings, enclosing sepsis and kidney transplantation [39,40,41]. It is characterized by renal blood flow blockage followed by reperfusion and re-oxygenation. This might be progressed to acute renal failure which correlates with high morbidity as well as death [42]. Renal failure is not usually the fundamental cause of mortality as it was suggested that injury of other organs can explain the outcome of patients [37]. Mortality among AKI patients complicated by multi-organ dysfunction stays high [43]. Till now, cardiovascular affection constitutes a main reason of AKI patients' mortality [44].

In CRS3, the AKI and cardiac malfunction interact in pathophysiologic pathways that are still insufficiently understood [45]. Nevertheless, new research has connected dysfunction of mitochondria to the pathogenesis of multiple kidney & cardiac disorders. Interestingly, the human body's greatest levels of mitochondria and oxygen utilization are found in the heart and kidney [46,47].

The current work established kidney I/R injury in male albino rats through renal ischemia bilaterally for 45 min, after that

reperfusion was restored. Male rats were chosen in this research to prevent cardioprotective impact of female hormones particularly when oxidative stress is present [48]. One week after renal I/R injury induction, rats of subgroup IIa (AKI subgroup) experienced a marked rise in urea along with creatinine concentrations versus sham-operated group. This agrees with prior work that documented a comparable significant elevation after 8 days of unilateral renal I/R injury in mice [49,50]. Buildup of uremic toxins due to inability of removing waste products generated from metabolism as urea and creatinine, represent a key indicator of renal impairment [51].

Previous research has established that the primary targets in the regulation of AKI-related cardiac dysfunction are the mitochondria-related cardiomyocyte bioenergetics [52]. Generation of ATP, production of ROS and regulation of the intrinsic pathway of apoptosis, are all essential functions of the mitochondria [53]. In light of the aforementioned data, the present work recorded a significant decrease in mitochondrial ATP level in AKI subgroup compared to control group, while mitochondrial H<sub>2</sub>O<sub>2</sub> level as well as the mean area percent of cytochrome C

immunoexpression, displayed a significant elevation.

Agreeing with these findings, CRS3 mice model has previously shown a considerable reduction in cardiomyocyte ATP generation, accompanied by higher levels of mitochondrial ROS, 3 days following I/R injury <sup>[54]</sup>. During ischemia, electron transport chain (ETC) exists in a reduced condition, while, after reperfusion, ETC combines with oxygen to produce ROS <sup>[55]</sup>; which increases mitochondrial permeability, leading to impaired function and, in turn, increased ROS formation <sup>[56]</sup>. Added to the previous findings, in a CRS3 model an increase in mitochondrial fragmentations was demonstrated <sup>[4]</sup>. It was suggested that alterations in mitochondrial morphology could prevent oxidative phosphorylation resulting in depletion of intracellular ATP.

As mitochondria become fragmented, cytochrome C leaks through the outer membrane of mitochondria and is regarded as the principal trigger of caspase cascade <sup>[37]</sup>. Mitochondrial malfunction formerly assessed in mice hearts subjected to renal I/R injury, has demonstrated fragmentation 1 day after injury, and increased caspase-3 activity and cytochrome C release into cardiomyocytes cytosol after 3 days detected

by Western blot analysis, indicating stimulation of apoptosis <sup>[57]</sup>.

The preceding data correlates with the present histological cardiac muscle alterations detected in AKI subgroup, focal areas of degeneration in some muscle fibers in the form of disrupted myofibrils and transverse striations, interrupted intercalated discs, along with darkly stained shrunken nuclei. This might be attributed to the renal ischemia resulting in elevated oxidative stress marker (H<sub>2</sub>O<sub>2</sub>) that react with biomolecules causing deoxyribonucleic acid cleavage (nuclear condensation and pyknosis), degradation of sarcoplasmic myofibrils and cardiac junction proteins and finally initiation of an apoptotic cascade. In light of this picture, a former study <sup>[58]</sup> illustrated similar early histological cardiac changes induced by kidney I/R. Likewise, the current experiment also spotted inflammatory cell infiltrations within widened endomysium which were in line with a former CRS3 model that attributed myocardial edema to the inflammatory reaction and considered it to be one of the mechanisms underlying cardiac dysfunction triggered by AKI <sup>[3]</sup>.

Resonating with these histological findings, in the present work, cardiac levels

of TNF- $\alpha$  in AKI subgroup recorded a significant rise in relation to control group. In support of this result, prior studies have found, following one week of kidney I/R, a maximum rise in pro-inflammatory cytokines, TNF- $\alpha$ , interleukin 1 beta (IL-1 $\beta$ ) as well as interferon gamma (IFN- $\gamma$ ) [59] in conjunction with elevated cardiac cell damage [60]. This was similarly reported in other models of renal I/R injury, where serum and cardiac inflammatory cytokines elevated 8 days later, while hypertrophy biomarkers increased after 15 days of the injury [59,61]. Correlating with the former outcomes, in the current research, the occurrence of inflammatory infiltration is suggested to activate fibroblast proliferation and differentiation to myofibroblast with subsequent collagen deposition. This was emphasized by the reported non-significant rise in the mean area percent of collagen fibers in AKI subgroup versus group I. This suggestion was in line with documentation of a former study [61]. It observed that inflammation might modulate heart tissue structure and regulate collagen amount in mice subjected to kidney I/R.

Inflammatory cascades that result in cell death and cardiac dysfunction is triggered by mitochondrial ROS [55], which, as mentioned earlier, was increased in the

heart in renal I/R injury [45]. Mitophagy, a chief regulator of mitochondrial homeostasis, is considered as the most effective method for removing intracellular ROS [62].

On that account, the most crucial mechanism for detecting mitochondria during cellular stress is PINK1/PARKIN-mediated mitophagy. When PINK1/PARKIN is ubiquitinated, it recruits the receptor protein P62/ sequestosome 1 (SQSTM1), that connects the ubiquitin-labeled mitochondria with LC3 in the autophagosome's membrane, resulting in removal of damaged mitochondria [63,64]. Throughout autophagy, LC3-I is transformed into LC3-II, subsequently, the level of LC3-II reflects the autophagosomes count [65]. P62, as a cargo receptor for autophagy, is considered the main defence protein controlling the autophagic destruction of mitochondrial remnants after oxidative stress [66]. Unfragmented autophagosomes are released outside of the cells as exosomes, which trigger inflammatory processes that damage mitochondria, exacerbate ROS buildup, prevent autophagosome breakdown, which finally create a pathophysiological vicious cycle [67]. This offers further explanation to the significant rise in H<sub>2</sub>O<sub>2</sub> level in AKI subgroup.

Correlating with the above-described pathway, in the current research, a non-significant elevation in mRNA expression of PINK1/PARKIN levels and the mean area percent of LC3IIB immunoreaction in cardiac fibers was detected in AKI subgroup when compared to group I. However, the mean area percent of P62 immunoexpression presented a significant rise in AKI subgroup versus control. An adaptive increase of autophagy might constitute an explanation to the former results, as the increase in LC3IIB, being non-significant, implies that the oxidative stress condition in the cardiomyocytes is beyond the capacity of autophagy process to overcome. This justifies the significant high level of P62, reflecting the shortfall of its degradation.

Levels of PINK1 and PARKIN in kidney were previously estimated, by immunoblotting, to be significantly increased 3 days following cisplatin-induced kidney injury [68]. As well, in a former study, a significant increase in LC3B level through immunohistochemical staining 2 weeks after acute myocardial infarction was recorded [69]. On the contrary, in an AKI model by cisplatin [70], the authors found after 3 days, a significant decrease in renal levels of LC3 II/LC3 I, PINK1, in addition to PARKIN measured by Western blotting. Meanwhile, in

consistence with our findings, P62 levels recorded a significant rise. The variations presented among the formerly mentioned studies could be attributed to differences in modalities, type and severity of tissue injury, species in addition to age of animals used, or duration of the study.

The induced mitophagy in AKI subgroup was supported by the SIRT-3 upregulation illustrated in the current work as a non-significant increase versus group I. As formerly reported, SIRT-3 enhances the upregulation of the PINK1-PARKIN pathway of mitophagy to prevent apoptosis [19]. Similarly in diabetic cardiomyopathy models [71,72], an activation of SIRT-3 was demonstrated to enhance PARKIN expression which retrieves mitophagy, alleviates oxidative stress, and preserves normal mitochondria synthesis [72].

Sirtuin-3 (SIRT-3), a NAD<sup>+</sup>-dependent protein deacetylase, [18] is strongly present in the mitochondria of heart tissues [73] and activated by oxidative stress [74]. It is noteworthy that SIRT-3 deacetylates both Mn-SOD [21] and peroxisome proliferator-activated receptor gamma coactivator 1 alpha (PGC1 $\alpha$ ) [20]. Manganese superoxide dismutase (Mn-SOD) represents a key enzyme for maintaining redox homeostasis

through scavenging superoxide in the mitochondria [75,76]. By deacetylation and activation of Mn-SOD, SIRT-3 has a significant effect in pathological cardiac remodeling; through its antioxidant effect [21,77]. Notably, SIRT-3 deacetylates PGC1 $\alpha$ , that exists abundantly in heart tissues, and upregulates its expression in stressful conditions [78] to enhance mitochondrial biogenesis in AKI [20]. This offers an explanation for the non-significant rise detected in the mean area percent of SIRT-3 immunoreactivity, mitochondrial Mn-SOD as well as the mRNA expression of PGC1 $\alpha$ , versus the control group. This non-significant enhancement might be linked to the previously recorded significant rise in the mitochondrial H<sub>2</sub>O<sub>2</sub> level, and the impairment of oxidant/antioxidant balance manifested by AKI subgroup.

Subgroup Iib (AKI/recovery subgroup) was designed to explore the influence of a recovery period on heart tissue. Thus, rats of this subgroup were sacrificed 4 weeks after AKI induction. Their serum urea and creatinine levels showed significant rise versus control group along with non-significant decrease in comparison to AKI subgroup. Similarly, previous investigators recorded elevated serum urea in ischemia group compared to sham rats after four weeks

of left renal artery and vein clamping for 60 minutes [79]. This uremic metabolic disturbance along with the inflammatory stimulation are linked to AKI-triggered cardiac injury [1].

Several pathological processes, including lipid peroxidation, enzyme denaturation, and DNA damage are triggered by ROS in the hypoxia/reoxygenation state [80]. All these processes are suggested to contribute to the persistence of myocardial damage in AKI/recovery subgroup. This was backed the significant increase in mitochondrial H<sub>2</sub>O<sub>2</sub> levels, and subsequently the mean area percent of cytochrome C immunostaining, along with significant drop in mitochondrial levels of ATP in AKI/recovery subgroup versus control group. In addition to the recorded non-significant difference versus AKI subgroup.

An exacerbated histological picture of cardiac tissue alterations was demonstrated in multiple muscle fibers in AKI/recovery subgroup, depicted as sarcoplasmic areas of degeneration with lost transverse striations, disrupted intercalated discs and pyknotic nuclei. This might be attributed to the conducted renal ischemia reperfusion injury which was bilateral; acting as a major factor contributing to the elevated mitochondrial

H<sub>2</sub>O<sub>2</sub> resulting in persistent cardiac affection. Additionally widened endomysium was seen in sections of AKI/recovery subgroup. It was occupied by inflammatory cells, fibroblasts like cells, in addition to collagen fibers deposition that exhibited a significant rise in the mean area percent versus group I and AKI subgroup displayed by Masson's trichrome staining. Parallel with this picture, TNF- $\alpha$  cardiac levels displayed a non-significant decrease in relation to AKI subgroup, yet a significant rise versus control group.

Going with these preceding findings, cardiac tissue sections studied 4 weeks after AKI in mice recorded cardiac inflammation, fibrosis, and cardiac dysfunction<sup>[81]</sup>. Further support documented in a previous study where cardiac fibrosis was encountered 4 weeks after I/R-AKI in mice<sup>[82]</sup>. Moreover, progressive cardiac and kidney failure is reported to be primarily mediated by long-term heart hypertrophy and cardiorenal fibrosis. This could be elucidated by the significant role that transforming growth factor-  $\beta$ 1 (TGF- $\beta$ 1) plays in fibrosis process especially in the heart and kidney<sup>[83,84]</sup>. It was previously reported that, macrophages, which eliminate necrotic cardiomyocytes<sup>[85]</sup>, become able to activate fibroblasts via TGF- $\beta$ 1-dependent manner<sup>[86]</sup>, leading to suppression of the inflammatory response and promotion of fibroblast's transformation into myofibroblasts<sup>[87]</sup>.

Myofibroblasts overproduce collagen causing fibrosis following I/R injury<sup>[88]</sup>. This could explain the recorded significant increase in collagen deposition of AKI/recovery subgroup versus the AKI subgroup in the current work.

Regarding the relative mRNA expressions of PINK1 and PARKIN and mean area percent of LC3IIB immunoeexpression, AKI/recovery subgroup recorded a significant reduction in comparison to AKI subgroup and control. On the other hand, the mean area percent of P62 immunoreactivity displayed a significant elevation. In accordance with our results, following acute myocardial infarction induction, at week 2 through 4, it was found that, in cardiac and renal tissues, LC3-II changed from a significant elevation to a minimal rise, and P62 altered from a non-evident increase to a significant elevation; as at week 4, the autophagy was inefficient<sup>[69]</sup>. Moreover, in a former study, by immunoblotting, renal PINK1 and PARKIN as well as LC3 levels were found to be significantly decreased 38 days after cisplatin-induced kidney injury<sup>[68]</sup>. Likewise, PINK1 as well as PARKIN expression was decreased, and that of P62 was elevated in cardiac mitochondria

following 4 weeks of myocardial ischemia-induced heart failure [89].

It has been hypothesized that persistent oxidative stress can damage lysosomes, inactivate autophagy, and trigger the cell death pathway [69]. Therefore, the increase of P62 is considered as a marker for suppression of autophagy or abnormalities in autophagic breakdown [90]. Another suggestion for the decreased mitophagy markers, and the increased P62 was linked to elevated apoptosis rate 4 weeks, relative to 2 weeks of acute myocardial infarction [69]. It was reported that continuous cell stress causes the apoptotic signals to be activated, which makes it unable to induce autophagy [91].

The Mn-SOD activity, mRNA expression of PGC1 $\alpha$  along with mean area percent of SIRT-3 immunostaining in AKI/recovery subgroup, detected a significant reduction as compared to AKI subgroup & control. The downregulation of SIRT-3 has been proven to impair oxidative phosphorylation and consequently imbalance of cardiomyocytes energy metabolism [92]. Being substantially related to mitochondrial damage [93], SIRT-3 contributes to antioxidant defense and mitochondrial ROS scavenging [21]. This links the drop detected in the levels of SIRT-3, Mn-SOD and ATP in

AKI/recovery subgroup, as well as the rise in H<sub>2</sub>O<sub>2</sub>, all together. Along those lines, elevated oxidative stress and mitochondrial dysfunction were previously reported to be associated with suppressed PGC1 $\alpha$  expression in heart failure [94].

Lately, studies have revealed favorable impact of EMPA, the SGLT2i, on the kidney and heart, playing an interesting part in attenuation of mitochondrial dysfunction. Fortunately, in non-diabetic normoglycemic people, EMPA causes only minimal urine glucose excretion and insignificant decrease of circulatory glucose levels. Therefore, hypoglycemia is uncommon [95]. This could be explained by EMPA's glucose lowering activity being proportionate to the blood glucose level and glomerular filtration rate [22]. Thus, EMPA was the drug of choice in this study to navigate its effect on rat model of CRS3 and explore its role in mitochondrial quality control.

To test the potential ameliorative influence of EMPA on the heart in CRS3, rats of subgroup IIc (AKI/EMPA subgroup) were treated with EMPA, starting one week after AKI induction and continued for three weeks. Their urea and creatinine levels showed a significant reduction versus AKI/recovery subgroup, and also, a non-significant rise

versus group I. In prior research <sup>[96]</sup>, EPMA was administered 24 days after CRS induction in rats. By day 42 after CRS induction, EMPA had lowered the creatinine level in comparison to CRS group. This result denoted the potentiality of EMPA in preserving the renal function.

AKI/EMPA subgroup's mitochondrial level of ATP displayed a significant increase versus AKI/recovery subgroup, and significant diminution versus control group. In contrast, mitochondrial H<sub>2</sub>O<sub>2</sub> measurements and cytochrome C immunoreactivity detected a significant decrease versus AKI/recovery, and a significant rise in relation to control. Parallel to these findings, EMPA treatment has shown to be able to preserve mitochondrial integrity through stabilization of their membrane potential; and thereby suppress ROS generation and increase levels of mitochondrial ATP in cardiomyocytes. This was recorded in different models such as CRS <sup>[54]</sup>, regional myocardial ischemia <sup>[97]</sup> and cardiac arrest induction <sup>[98]</sup>. A Similar pattern was found in a former study <sup>[96]</sup> where EMPA treatment in CRS rat model resulted in decrease in caspase-3 and cytosolic cytochrome C by Western blotting.

An improvement in cardiac muscle histological alterations was observed in

AKI/EMPA subgroup. Although, pyknotic nuclei, scarce focal areas of degeneration in some muscle fibers and very few inflammatory cells in the endomysium were spotted. Associating with this analysis, TNF- $\alpha$  cardiac levels recorded significant decrease in relation to AKI/recovery subgroup, along with a non-significant increase versus group I; this might account for the preceding ameliorated histological outcome. As for Masson 's trichrome staining, a significant diminution in the mean area percent of collagen fibers in relation to AKI/recovery subgroup and non-significant elevation versus control was displayed which matched the inflammatory condition.

In line with the former data, EPMA administration in rat CRS model <sup>[96]</sup> demonstrated reduced myocardial inflammatory indicators; TNF- $\alpha$ , IL-1 $\beta$  & nuclear factor kappa (NF- $\kappa$ B), as well as decrease in Masson's trichrome-stained fibrotic area in the myocardium. This might be attributed to the reduction of TGF- $\beta$ . Furthermore, EMPA treatment has diminished the myocardial injury, cardiac dysfunction, and fibrosis in cardiac arrest rat model <sup>[98]</sup>.

In the present work, conforming to the fact that triggering mitophagy shields

cells against malfunction of the mitochondria and cell damage <sup>[99]</sup>, mRNA expression of PINK1 and PARKIN and the mean area percent of LC3IIB immunoreactivity showed a significant elevation in AKI/EMPA subgroup as compared to AKI/recovery subgroup and significant decrease compared to control group. As for the mean area percent of P62 immunostaining, AKI/EMPA subgroup displayed a significant decline versus AKI/recovery subgroup and significant rise versus control group. Supporting the aforementioned findings, it was previously illustrated that EMPA administration, markedly improved LC3-II/LC3-I ratio in renal ischemia reperfusion injury <sup>[100]</sup> and doxorubicin-induced cardiomyopathy model <sup>[101]</sup>, as well as increased LC3-II and decreased P62 expression in diabetic tubulopathy model <sup>[65]</sup>, reflecting its ability to enhance the autophagic flux.

Regarding Mn-SOD level, mean area percent of SIRT-3 positive immunoreaction and mRNA expression of PGC1 $\alpha$ , AKI/EMPA subgroup showed a significant elevation versus AKI/recovery subgroup and significant decline versus control group. EMPA treatment for 14 days before myocardial infarction was shown to enhance the expression of antioxidant stress proteins,

SOD2 levels and lower the oxidative stress indicators in the rats <sup>[102]</sup> which is compatible with our findings. Furthermore, in a prior study, rats treated with EMPA had considerably higher levels of the protein SIRT-3, which is involved in the activation of SOD2 as previously noted <sup>[103]</sup>. Along those lines, PGC1 $\alpha$  levels were shown to be upregulated by EMPA treatment in renal I/R injury <sup>[100]</sup>. The former data delivers a notable interconnection between the cardiomyocyte mitochondrial oxidant/antioxidants homeostasis, mitophagy/mitochondrial biogenesis, and the capability of EMPA treatment to enhance both.

## **5. Conclusion:**

Cardiorenal syndrome type 3 defines an intersection where AKI induces cardiac muscle damage. Mechanisms through which AKI impairs the heart comprise the accumulation of uremic toxins, oxidative stress, cardiac energy deficit, myocardial inflammation, fibrosis, cardiomyocyte apoptosis and dysregulated mitochondrial homeostasis. The promising effects of EMPA on the heart revolve around enhancing cardiac energy metabolism and decreasing pathological remodeling, directed primarily by EMPA's key contribution to mitochondrial quality control process.

**Recommendations:**

From the current study, it is recommended to administer EMPA to AKI susceptible individuals as early as possible. Nonetheless, further study is required to provide more clarification of the underlying pathophysiological processes of CRS3 and to validate more clarification of EMPA's different mechanisms preserving the cardiac structure and function.

**Conflict of interests:**

There are no conflicts of interest.

**6. References:**

- 1- Rangaswami J, Bhalla V, Blair JEA, Chang TI, Costa S, Lentine KL, Lerma EV, Mezue K, Molitch M, Mullens W, Ronco C, Tang WHW, McCullough PA; American Heart Association Council on the Kidney in Cardiovascular Disease and Council on Clinical Cardiology. Cardiorenal Syndrome: Classification, Pathophysiology, Diagnosis, and Treatment Strategies: A Scientific Statement from the American Heart Association. *Circulation*. 2019;139:e840-e878.
- 2- Lullo DL, Reeves RB, Bellasi A, Ronco C. Cardiorenal Syndrome in Acute Kidney Injury. *Semin. Nephrol*. 2019; 39: 31–40.
- 3- Wang J, Toan S, Li R, Zhou H. Melatonin fine-tunes intracellular calcium signals and eliminates myocardial damage through the IP3R/MCU pathways in cardiorenal syndrome type 3. *Biochemical Pharmacology*. 2020; 174: Article ID 113832, 1-10.
- 4- Wang J, Sun X, Wang X, Cui S, Liu R, Liu J, Fu B, Gong M, Wang C, Shi Y, Chen Q, Cai G, Chen X. Grb2 Induces Cardiorenal Syndrome Type 3: Roles of IL-6, Cardiomyocyte Bioenergetics, and Akt/mTOR Pathway. *Frontiers in Cell and Developmental Biology*. 2021; 9: Article ID 630412, 1-15.
- 5- Du Y, Li X, Liu B. Advances in pathogenesis and current therapeutic strategies for cardiorenal syndrome. *Life Sciences*. 2014;99: 1–6.
- 6- Lazarou M, Sliter DA, Kane LA, Sarraf SA, Wang C, Burman JL, Sideris DP, Fogel AI, Youle RJ. The ubiquitin kinase PINK1 recruits autophagy receptors to induce mitophagy. *Nature*. 2015; 524:309-314.
- 7- Dorn GW. Parkin-dependent mitophagy in the heart. *J. Mol. Cell. Cardiol*. 2016; 95, 42–49.
- 8- Riley BE, Loughheed JC, Callaway K, Velasquez M, Brecht E, Nguyen L, Shaler T, Walker D, Yang Y, Regnstrom K, Diep L, Zhang Z, Chiou S, Bova M,

- Artis DR, Yao N, Baker J, Yednock T, Johnston JA. Structure and function of Parkin E3 ubiquitin ligase reveals aspects of RING and HECT ligases. *Nat Commun.* 2013; 4: Article ID 1982,1-9.
- 9- Rojansky R, Cha MY, Chan DC. Elimination of paternal mitochondria in mouse embryos occurs through autophagic degradation dependent on PARKIN and MUL1. *Elife.* 2016;5: Article ID e17896,1-18.
- 10- Livingston MJ, Wang J, Zhou J, Wu G, Ganley IG, Hill JA, Yin XM, Dong Z. Clearance of damaged mitochondria via mitophagy is important to the protective effect of ischemic preconditioning in kidneys. *Autophagy.* 2019; 15:2142-2162.
- 11- Tang C, Han H, Yan M, Zhu S, Liu J, Liu Z, He L, Tan J, Liu Y, Liu H, Sun L, Duan S, Peng Y, Liu F, Yin XM, Zhang Z, Dong Z. PINK1-PRKN/PARK2 pathway of mitophagy is activated to protect against renal ischemia-reperfusion injury. *Autophagy.* 2018; 14:880-897.
- 12- Wang Y, Tang C, Cai J, Chen G, Zhang D, Zhang Z, Dong Z. PINK1/Parkin-mediated mitophagy is activated in cisplatin nephrotoxicity to protect against kidney injury. *Cell Death Dis.* 2018; 9: Article ID 1113,1-14.
- 13- Wang S, Chen Y, Li X, Zhang W, Liu Z, Wu M, Pan Q, Liu H. Emerging role of transcription factor EB in mitochondrial quality control. *Biomed Pharmacother.* 2020; 128: Article ID 110272,1-10.
- 14- Karamanlidis G, Nascimben L, Couper GS, Shekar PS, del Monte F, Tian R. Defective DNA replication impairs mitochondrial biogenesis in human failing hearts. *Circ Res.* 2010; 106:1541–1548.
- 15- Dominy JE, Puigserver P. Mitochondrial biogenesis through activation of nuclear signaling proteins. *Cold Spring Harb Perspect Biol.* 2013; 5: Article ID a015008,1-18.
- 16- Wang Y, Zhu J, Liu Z, Shu S, Fu Y, Liu Y, Cai J, Tang C, Liu Y, Yin X, Dong Z. The PINK1/PARK2/optineurin pathway of mitophagy is activated for protection in septic acute kidney injury. *Redox Biol.* 2021; 38: Article ID 101767,1-16.
- 17- Wang C, Wang Y, Shen L. Mitochondrial proteins in heart failure: the role of deacetylation by SIRT3. *Pharmacol Res.* 2021;172: Article ID 105802, 1-12.
- 18- Koentges C, Pfeil K, Schnick T, Wiese S, Dahlbock R, Cimolai MC, Meyer-Steenbuck M, Cenkerova K, Hoffmann MM, Jaeger C, Odening KE, Kammerer B, Hein L, Bode C, Bugger H. SIRT3 deficiency impairs mitochondrial and

- contractile function in the heart. *Basic Res Cardiol.* 2015; 110: Article ID 36,1-20.
- 19- Li Y, Ma Y, Song L, Yu L, Zhang L, Zhang Y, Xing Y, Yin Y, Ma H. SIRT3 deficiency exacerbates p53/Parkin - mediated mitophagy inhibition and promotes mitochondrial dysfunction: implication for aged hearts. *Int J Mol Med.* 2018; 41: 3517- 3526.
- 20- Morigi M, Perico L, Benigni A. Sirtuins in renal health and disease. *J Am Soc Nephrol.* 2018; 29: 1799- 1809.
- 21- Liu J, Li D, Zhang T, Tong Q, Ye RD, Lin L. SIRT3 protects hepatocytes from oxidative injury by enhancing ROS scavenging and mitochondrial integrity. *Cell Death Dis.* 2017;8: Article ID e3158, 1-11.
- 22- Thomas MC, Cherney DZI. The actions of SGLT2 inhibitors on metabolism, renal function and blood pressure. *Diabetologia.* 2018; 61: 2098–2107.
- 23- Martens P, Mathieu C, Verbrugge FH. Promise of SGLT2 inhibitors in heart failure: diabetes and beyond. *Curr Treat Options Cardiovasc Med* 2017; 19: Article ID 23,1-14.
- 24- Chen J, Fan F, Wang JY, Long Y, Gao CL, Stanton RC, Xu Y. The efficacy and safety of SGLT2 inhibitors for adjunctive treatment of type 1 diabetes: a systematic review and meta-analysis. *Sci Rep.* 2017; 7: Article ID 44128,1-9.
- 25- Yurista SR, Silljé HHW, Oberdorf-Maass SU, Schouten EM, Pavez Giani MG, Hillebrands JL, van Goor H, van Veldhuisen DJ, de Boer RA, Westenbrink BD. Sodium-glucose co-transporter 2 inhibition with empagliflozin improves cardiac function in nondiabetic rats with left ventricular dysfunction after myocardial infarction. *Eur J Heart Fail* 2019; 21:862–873.
- 26- Steven S, Oelze M, Hanf A, Kröller-Schön S, Kashani F, Roohani S, Welschhof P, Kopp M, Gödtel-Armbrust U, Xia N, Li H, Schulz E, Lackner KJ, Wojnowski L, Bottari SP, Wenzel P, Mayoux E, Münzel T, Daiber A. The SGLT2 inhibitor empagliflozin improves the primary diabetic complications in ZDF rats. *Redox Biol.* 2017; 13:370-385.
- 27- Al-Jobori H, Daniele G, Cersosimo E, Triplitt C, Mehta R, Norton L, DeFronzo RA, Abdul-Ghani M. Empagliflozin and kinetics of renal glucose 2 transport in healthy individuals and individuals with type 2 diabetes. *Diabetes.*2017; 66:1999–2006.
- 28- Hu Z, Ju F, Du L, Abbott GW. Empagliflozin protects the heart against ischemia/reperfusion-induced sudden

- cardiac death. *Cardiovasc Diabetol.* 2021; 20: Article ID 199,1-13.
- 29- Caio-Silva W, da Silva Dias D, Junho CVC, Panico K, Neres-Santos RS, Pelegrino MT, Pieretti JC, Seabra AB, De Angelis K, Carneiro-Ramos MS. Characterization of the Oxidative Stress in Renal Ischemia/Reperfusion-Induced Cardiorenal Syndrome Type 3. *BioMed Res. Int.* 2020; 2020: Article ID 1605358,1-11.
- 30- Lima NKS, Farias WRA, Cirilo MAS, Oliveira AG, Farias JS, Aires RS, Muzi-Filho H, Paixão ADO, Vieira LD. Renal ischemia-reperfusion leads to hypertension and changes in proximal tubule  $\text{Na}^+$  transport and renin-angiotensin-aldosterone system: Role of NADPH oxidase. *Life Sci.* 2021; 266: Article ID 118879,1-9.
- 31- Pechman KR, De Miguel C, Lund H, Leonard EC, Basile DP, Mattson DL. Recovery from renal ischemia-reperfusion injury is associated with altered renal hemodynamics, blunted pressure natriuresis, and sodium-sensitive hypertension. *Am J Physiol Regul Integr Comp Physiol.* 2009; 297: R1358-R1363.
- 32- El Agaty SM. Cardioprotective effect of vitamin D2 on isoproterenol-induced myocardial infarction in diabetic rats. *Archives of Physiology and Biochemistry.* 2019; 125:210- 219.
- 33- Gumustaz K, Tanrived T, Kulaksiz I, Kafadar AM, Sanus GZ, Atukeren P, Kaynar MY. Cytochrome oxidase activity and ATP levels in high-grade gliomas and meningiomas. *Turk Neurosurg.* 2006;16: 64.
- 34- Li S, Lin Q, Shao X, Zhu X, Wu J, Wu B, Zhang M, Zhou W, Zhou Y, Jin H, Zhang Z, Qi C, Shen J, Mou S, Gu L, Ni Z. Drp1-regulated PARK2-dependent mitophagy protects against renal fibrosis in unilateral ureteral obstruction. *Free Radic Biol Med.* 2020; 152:632-649.
- 35- Suvarna K, Layton C, Bancroft J. The haematoxylin and eosin, Connective and mesenchymal tissue with their stains & Immunohistochemical and immunofluorescent techniques. In *Bancroft's Theory and Practice of Histological Techniques (Eighth Edition)*, Elsevier, 2019, pp: 126-138, 153-175 & 337-394.
- 36- Liu JX, Yang C, Zhang WH, Su HY, Liu ZJ, Pan Q, Liu HF. Disturbance of mitochondrial dynamics and mitophagy in sepsis-induced acute kidney injury. *Life sciences.* 2019; 235: Article ID 116828,1-9.

- 37-Doi K. Kidney-Heart Interactions in Acute Kidney Injury. *Nephron* 2016; 134:141–144.
- 38-Emsley R, Dunn G and White IR. Mediation and moderation of treatment effects in randomized controlled trials of complex interventions. *Statistical Methods in Medical Research*; 2010;19: 237-270.
- 39-Gao Y, Zeng Z, Li T, Xu S, Wang X, Chen Z, Lin C. Polydatin inhibits mitochondrial dysfunction in the renal tubular epithelial cells of a rat model of sepsis-induced acute kidney injury. *Anesth. Analg.* 2015; 121: 1251–1260.
- 40-Benck U, Schnuelle P, Krüger B, Nowak K, Riester T, Mundt H, Lutz N, Jung M, Birck R, Krämer BK, Schmitt WH. Excellent graft and patient survival after renal transplantation from donors after brain death with acute kidney injury: A case-control study. *Int. Urol. Nephrol.* 2015; 47: 2039–2046.
- 41-Zhu YB, Zhang YP, Zhang J, Zhang YB. Evaluation of Vitamin C supplementation on kidney function and vascular reactivity following renal ischemic injury in mice. *Kidney Blood Press. Res.* 2016; 41: 460–470.
- 42-Sawhney S, Marks A, Fluck N, Levin A, Prescott G, Black C. Intermediate and Long-term Outcomes of Survivors of Acute Kidney Injury Episodes: A Large Population-Based Cohort Study. *Am. J. Kidney Dis.* 2017; 69: 18–28.
- 43-Grams ME, Rabb H. The distant organ effects of acute kidney injury. *Kidney Int.* 2012; 81: 942–948.
- 44-Wijerathne CUB, Madduma Hewage S, Siow YL, O K. Kidney Ischemia-Reperfusion Decreases Hydrogen Sulfide and Increases Oxidative Stress in the Heart. *Biomolecules.* 2020; 10: Article ID 1565,1-13.
- 45-Clementi A, Virzì GM, Brocca A, de Cal M, Pastori S, Clementi M, Granata A, Vescovo G, Ronco C. Advances in the pathogenesis of cardiorenal syndrome type 3. *Oxid Med Cell Longev.* 2015; 2015: Article ID 148082,1-8.
- 46-Zhang X, Agborbesong E, Li X. The Role of Mitochondria in Acute Kidney Injury and Chronic Kidney Disease and Its Therapeutic Potential. *Int. J. Mol. Sci.* 2021; 22: Article ID 11253,1-22.
- 47-Bhargava P, Schnellmann R.G. Mitochondrial energetics in the kidney. *Nat. Rev. Nephrol.* 2017; 13: 629–646.
- 48-Ryczkowska K, Adach W, Janikowski K, Banach M, Bielecka-Dabrowa A. Menopause and women's cardiovascular health: is it really an obvious relationship? *Arch Med Sci.* 2022; 19:458-466.

- 49- Neres-Santos RS, Junho CVC, Panico K, Caio-Silva W, Pieretti JC, Tamashiro JA, Seabra AB, Ribeiro CAJ, Carneiro-Ramos MS. Mitochondrial Dysfunction in Cardiorenal Syndrome 3: Renocardiac Effect of Vitamin C. *Cells*. 2021; Article ID 10:3029,1-14.
- 50- Junho CVC, González-Lafuente L, Neres-Santos RS, Navarro-García JA, Rodríguez-Sánchez E, Ruiz-Hurtado G, Carneiro-Ramos MS. Klotho relieves inflammation and exerts a cardioprotective effect during renal ischemia/reperfusion-induced cardiorenal syndrome. *Biomed Pharmacother*. 2022; 153: Article ID 113515,1-13.
- 51- Falconi CA, Junho CVDC, Fogaça-Ruiz F, Vernier ICS, da Cunha RS, Stinghen AEM, Carneiro-Ramos. Uremic Toxins: An Alarming Danger Concerning the Cardiovascular System. *Frontiers in physiology*. 2021; 12: Article ID 686249,1-20.
- 52- Husain-Syed F, Rosner MH, Ronco C. Distant organ dysfunction in acute kidney injury. *Acta Physiol*. 2020; 228: Article ID e13357,1-10.
- 53- Tanriover C, Copur S, Ucku D, Cakir AB, Hasbal NB, Soler MJ, Kanbay M. The Mitochondrion: A Promising Target for Kidney Disease. *Pharmaceutics*. 2023; 15: Article ID 570,1-30.
- 54- Cai C, Wu F, Zhuang B, Ou Q, Peng X, Shi N, Peng L, Li Z, Wang J, Cai S, Tan Y. Empagliflozin activates Wnt/ $\beta$ -catenin to stimulate FUNDC1-dependent mitochondrial quality surveillance against type-3 cardiorenal syndrome. *Mol Metab*. 2022; 64: Article ID 101553,1-14.
- 55- Moris D, Spartalis M, Spartalis E, Karachaliou GS, Karaolani GI, Tsourouflis G, Tsilimigras DI, Tzatzaki E, Theocharis S. The role of reactive oxygen species in the pathophysiology of cardiovascular diseases and the clinical significance of myocardial redox. *Ann Transl Med*. 2017; 5: Article ID 326,1-10.
- 56- Rubattu S, Mennuni S, Testa M, Mennuni M, Pierelli G, Pagliaro B, Gabriele E, Coluccia R, Autore C, Volpe M. Pathogenesis of chronic cardiorenal syndrome: is there a role for oxidative stress? *Int J Mol Sci*. 2013; 14:23011-23032.
- 57- Sumida M, Doi K, Ogasawara E, Yamashita T, Hamasaki Y, Kariya T, Takimoto E, Yahagi N, Nangaku M, Noiri E. Regulation of mitochondrial dynamics by dynamin-related protein-1 in acute cardiorenal syndrome. *J Am Soc Nephrol*. 2015; 26:2378-2387.

- 58- Youssef MI, Mahmoud AA, Abdelghany RH. A new combination of sitagliptin and furosemide protects against remote myocardial injury induced by renal ischemia/reperfusion in rats. *Biochem Pharmacol.* 2015; 96:20-29.
- 59- Trentin-Sonoda M, da Silva RC, Kmit FV, Abrahão MV, Monnerat Cahli G, Brasil GV, Muzi-Filho H, Silva PA, Tovar-Moll FF, Vieyra A, Medei E, Carneiro-Ramos MS. Knockout of Toll-Like Receptors 2 and 4 Prevents Renal Ischemia-Reperfusion-Induced Cardiac Hypertrophy in Mice. *PLoS One.* 2015;10: Article ID e0139350,1-21.
- 60- Junho CVC, González-Lafuente L, Navarro-García J A, Rodríguez-Sánchez E, Carneiro-Ramos MS, Ruiz-Hurtado G. Unilateral Acute Renal Ischemia-Reperfusion Injury Induces Cardiac Dysfunction through Intracellular Calcium Mishandling. *International journal of molecular sciences.* 2022; 23: Article ID 2266,1-15.
- 61- Cirino-Silva R, Kmit FV, Trentin-Sonoda M, Nakama KK, Panico K, Alvim JM, Dreyer TR, Martinho-Silva H, Carneiro-Ramos MS. Renal ischemia/reperfusion-induced cardiac hypertrophy in mice: Cardiac morphological and morphometric characterization. *JRSM Cardiovasc Dis.* 2017; 6: Article ID 2048004016689440,1-10
- 62- Dorn GW 2nd, Kitsis RN. The mitochondrial dynamism-mitophagy-cell death interactome: multiple roles performed by members of a mitochondrial molecular ensemble. *Circ Res.* 2015; 116:167-182.
- 63- Bueno M, Lai YC, Romero Y, Brands J, St Croix CM, Kanga C, Corey C, Herazo-Maya JD, Sembrat J, Lee JS, Duncan SR, Rojas M, Shiva S, Chu CT, Mora AL. PINK1 deficiency impairs mitochondrial homeostasis and promotes lung fibrosis. *J Clin Invest.* 2015; 125:521- 538.
- 64- Zimmermann M, Reichert AS. How to get rid of mitochondria: crosstalk and regulation of multiple mitophagy pathways. *Biol Chem.* 2017; 399:29-45.
- 65- Lee YH, Kim SH, Kang JM, Heo JH, Kim DJ, Park SH, Sung M, Kim J, Oh J, Yang DH, Lee SH, Lee SY. Empagliflozin attenuates diabetic tubulopathy by improving mitochondrial fragmentation and autophagy. *Am J Physiol Renal Physiol.* 2019; 317: F767-F780.
- 66- Pugsley HR. Assessing autophagic flux by measuring LC3, p62, and LAMP1 colocalization using multispectral imaging flow cytometry. *J Vis Exp.* 2017; 125: Article ID 55637,1-13.

- 67- Zeng X, Zhang YD, Ma RY, Chen YJ, Xiang XM, Hou DY, Li XH, Huang H, Li T, Duan CY. Activated Drp1 regulates p62-mediated autophagic flux and aggravates inflammation in cerebral ischemia-reperfusion via the ROS-RIP1/RIP3-exosome axis. *Mil Med Res.* 2022; 9: Article ID 25,1-17.
- 68- Ma N, Wei Z, Hu J, Gu W, Ci X. Ferrerol Ameliorated Cisplatin-Induced Chronic Kidney Disease Through Mitophagy Induction via Nrf2/PINK1 Pathway. *Front Pharmacol.* 2021; 12: Article ID 768700,1-15.
- 69- Feng Z, Jiang HX, Chen H, Liu YN, Wang Y, Yang RB, Han X, Xia CH, Zhu ZB, Shang H, Wu A, Liu WJ. Adaptive Autophagy Offers Cardiorenal Protection in Rats with Acute Myocardial Infarction. *Cardiol Res Pract.* 2020; 2020: Article ID 7158975,1-10.
- 70- Qi J, Xue Q, Kuang L, Xie L, Luo R, Nie X. Berberine alleviates cisplatin-induced acute kidney injury by regulating mitophagy via PINK 1/Parkin pathway. *Transl Androl Urol.* 2020; 9:1712-1724.
- 71- Wang S, Zhao Z, Fan Y, Zhang M, Feng X, Lin J, Hu J, Cheng Z, Sun C, Liu T, Xiong Z, Yang Z, Wang H, Sun D. Mst1 inhibits Sirt3 expression and contributes to diabetic cardiomyopathy through inhibiting Parkin-dependent mitophagy. *Biochim Biophys Acta Mol Basis Dis.* 2019; 1865:1905-1914.
- 72- Yu W, Gao B, Li N, Wang J, Qiu C, Zhang G, Liu M, Zhang R, Li C, Ji G, Zhang Y. Sirt3 deficiency exacerbates diabetic cardiac dysfunction: Role of Foxo3A-Parkin-mediated mitophagy. *Biochim Biophys Acta Mol Basis Dis.* 2017; 1863:1973-1983.
- 73- Peng S, Lu XF, Qi YD, Li J, Xu J, Yuan TY, Wu XY, Ding Y, Li WH, Zhou GQ, Wei Y, Li J, Chen SW, Liu SW. LCZ696 Ameliorates Oxidative Stress and Pressure Overload-Induced Pathological Cardiac Remodeling by Regulating the Sirt3/MnSOD Pathway. *Oxid Med Cell Longev.* 2020; 2020: Article ID 9815039,1-15.
- 74- Shi T, Wang F, Stieren E and Tong Q: SIRT3, a mitochondrial sirtuin deacetylase, regulates mitochondrial function and thermogenesis in brown adipocytes. *J Biol Chem.* 2005; 280: 13560-13567.
- 75- He H, Tao H, Xiong H, Duan SZ, McGowan FX Jr, Mortensen RM, Balschi JA. Rosiglitazone causes cardiotoxicity via peroxisome proliferator-activated receptor  $\gamma$ -independent mitochondrial oxidative stress in mouse hearts. *Toxicol Sci.* 2014; 138:468- 481.

- 76- Kim T, Yang Q. "Peroxisome-proliferator-activated receptors regulate redox signaling in the cardiovascular system," *World Journal of Cardiology*. 2013; 5: 164–174.
- 77- Tao R, Coleman MC, Pennington JD, Ozden O, Park SH, Jiang H, Kim HS, Flynn CR, Hill S, Hayes McDonald W, Olivier AK, Spitz DR, Gius D. Sirt3-mediated deacetylation of evolutionarily conserved lysine 122 regulates MnSOD activity in response to stress. *Mol Cell*. 2010; 40:893-904.
- 78- Chen L, Qin Y, Liu B, Gao M, Li A, Li X, Gong G. PGC-1 $\alpha$ -Mediated Mitochondrial Quality Control: Molecular Mechanisms and Implications for Heart Failure. *Front Cell Dev Biol*. 2022; 10: Article ID 871357,1-12.
- 79- Buys-Gonçalves GF, Sampaio FJB, Silva MEM, Pereira-Sampaio MA, De Souza DB. Histomorphometric evaluation of the rat kidney submitted to warm ischemia and the protective effect of resveratrol. *American journal of surgery*. 2020; 220: 1119–1123.
- 80- Yang M, Xi N, Gao M, Yu Y. Sitagliptin mitigates hypoxia/reoxygenation (H/R)-induced injury in cardiomyocytes by mediating sirtuin 3 (SIRT3) and autophagy. *Bioengineered*. 2022; 13:13162-13173.
- 81- Prud'homme M, Coutrot M, Michel T, Boutin L, Genest M, Poirier F, Launay JM, Kane B, Kinugasa S, Prakoura N, Vandermeersch S, Cohen-Solal A, Delcayre C, Samuel JL, Mehta R, Gayat E, Mebazaa A, Chadjichristos CE, Legrand M. Acute Kidney Injury Induces Remote Cardiac Damage and Dysfunction Through the Galectin-3 Pathway. *JACC Basic Transl Sci*. 2019; 4:717-732.
- 82- Florens N, Kasam RK, Rudman-Melnick V, Lin SC, Prasad V, Molkentin JD. Interleukin-33 Mediates Cardiomyopathy After Acute Kidney Injury by Signaling to Cardiomyocytes. *Circulation*. 2023; 147:746-758.
- 83- Han WK, Alinani A, Wu CL, Michaelson D, Loda M, McGovern FJ, Thadhani R, Bonventre JV. Human kidney injury molecule-1 is a tissue and urinary tumor marker of renal cell carcinoma. *J Am Soc Nephrol*. 2005; 16:1126- 1134.
- 84- Yanagita M. Inhibitors/antagonists of TGF-beta system in kidney fibrosis. *Nephrol Dial Transpl*. 2012; 27:3686–3691
- 85- Lamberti Y, Perez Vidakovics ML, van der Pol LW, Rodríguez ME. Cholesterol-rich domains are involved in Bordetella pertussis phagocytosis and intracellular

- survival in neutrophils. *Microb Pathog.* 2008; 44:501-511.
- 86- Sun Y, Zhang JQ, Zhang J, Lamparter S. Cardiac remodeling by fibrous tissue after infarction in rats. *J Lab Clin Med.* 2000; 135:316- 323.
- 87- Wynn TA. Cellular and molecular mechanisms of fibrosis. *J Pathol.* 2008; 214: 199–210
- 88- Talman V, Ruskoaho H. Cardiac fibrosis in myocardial infarction-from repair and remodeling to regeneration. *Cell Tissue Res.* 2016; 365:563-581.
- 89- Hu J, Liu T, Fu F, Cui Z, Lai Q, Zhang Y, Yu B, Liu F, Kou J, Li F. Omentin1 ameliorates myocardial ischemia-induced heart failure via SIRT3/FOXO3a-dependent mitochondrial dynamical homeostasis and mitophagy. *J Transl Med.* 2022; 20: Article ID 447,1-21.
- 90- Bjørkøy G, Lamark T, Pankiv S, Øvervatn A, Brech A, Johansen T. Monitoring Autophagic Degradation of p62/SQSTM1. *Methods Enzymol.* 2009; 452: 181-197.
- 91- Kang R, Zeh HJ, Lotze MT, Tang D. The Beclin 1 network regulates autophagy and apoptosis. *Cell Death Differ.* 2011; 18:571- 580.
- 92- Zhang J, Xiang H, Liu J, Chen Y, He RR, Liu B. Mitochondrial Sirtuin 3: new emerging biological function and therapeutic target. *Theranostics.* 2020; 10:8315– 8342.
- 93- Singh CK, Chhabra G, Ndiaye MA, Garcia-Peterson LM, Mack NJ, Ahmad N. The Role of Sirtuins in Antioxidant and Redox Signaling. *Antioxid Redox Signal.* 2018; 28:643-661.
- 94- Gao YM, Feng ST, Wen Y, Tang TT, Wang B, Liu BC. Cardiorenal protection of SGLT2 inhibitors-Perspectives from metabolic reprogramming. *EBioMedicine.* 2022; 83: Article ID 104215,1-15.
- 95- Salvatore T, Galiero R, Caturano A, Rinaldi L, Di Martino A, Albanese G, Di Salvo J, Epifani R, Marfella R, Docimo G, Lettieri M, Sardu C, Sasso FC. An Overview of the Cardiorenal Protective Mechanisms of SGLT2 Inhibitors. *Int J Mol Sci.* 2022; 23: Article ID 3651,1-44.
- 96- Yang CC, Chen YT, Wallace CG, Chen KH, Cheng BC, Sung PH, Li YC, Ko SF, Chang HW, Yip HK. Early administration of empagliflozin preserved heart function in cardiorenal syndrome in rat. *Biomed Pharmacother.* 2019; 109:658-670.
- 97- Lu Q, Liu J, Li X, Sun X, Zhang J, Ren D, Tong N, Li J. Empagliflozin attenuates ischemia and reperfusion injury through LKB1/AMPK signaling pathway. *Mol*

- Cell Endocrinol. 2020; 501: Article ID 110642,1-11.
- 98- Tan Y, Yu K, Liang L, Liu Y, Song F, Ge Q, Fang X, Yu T, Huang Z, Jiang L, Wang P. Sodium-Glucose Co-Transporter 2 Inhibition with Empagliflozin Improves Cardiac Function After Cardiac Arrest in Rats by Enhancing Mitochondrial Energy Metabolism. *Front Pharmacol.* 2021; 12: Article ID 758080,1-12.
- 99- Zhao C, Chen Z, Xu X, An X, Duan S, Huang Z, Zhang C, Wu L, Zhang B, Zhang A, Xing C, Yuan Y. Pink1/Parkin-mediated mitophagy play a protective role in cisplatin induced renal tubular epithelial cells injury. *Exp Cell Res.* 2017; 350:390-397.
- 100- Ala M, Khoshdel MRF, Dehpour AR. Empagliflozin Enhances Autophagy, Mitochondrial Biogenesis, and Antioxidant Defense and Ameliorates Renal Ischemia/Reperfusion in Nondiabetic Rats. *Oxid Med Cell Longev.* 2022; 2022: Article ID 1197061,1-9.
- 101- Wang CY, Chen CC, Lin MH, Su HT, Ho MY, Yeh JK, Tsai ML, Hsieh IC, Wen MS. TLR9 Binding to Beclin 1 and Mitochondrial SIRT3 by a Sodium-Glucose Co-Transporter 2 Inhibitor Protects the Heart from Doxorubicin Toxicity. *Biology (Basel).* 2020; 9: Article ID 369,1-22.
- 102- Oshima H, Miki T, Kuno A, Mizuno M, Sato T, Tanno M, Yano T, Nakata K, Kimura Y, Abe K, Ohwada W, Miura T. Empagliflozin, an SGLT2 Inhibitor, Reduced the Mortality Rate after Acute Myocardial Infarction with Modification of Cardiac Metabolomes and Antioxidants in Diabetic Rats. *J Pharmacol Exp Ther.* 2019; 368:524-534.
- 103- Tseng AH, Wu LH, Shieh SS, and Wang DL. SIRT3 interactions with FOXO3 acetylation, phosphorylation and ubiquitinylation mediate endothelial cell responses to hypoxia. *Biochem J.* 2014; 464:157–168.